Development of improved superconductive axial gradiometers for biomagnetic SQUID applications

M. M. Budnyk[a)] and Yu. D. Minov

V.M. Glushkov Institute of Cybernetics, National Academy of Sciences of Ukraine, 40 Glushkov Ave., Kiev 03187, Ukraine

V. Yu. Lyakhno, V. A. Desnenko, and A. S. Linnik

B.I. Verkin Institute for Low Temperature Physics and Engineering, National Academy of Sciences of Ukraine, 47 Nauki Ave., Kharkov 61103, Ukraine

O. B. Shopen

Research and Production Enterprise Plastar Ltd., 8 Razin str., Zolochev, 62203 Kharkov, Ukraine

(Submitted November 7, 2017)
Fiz. Nizk. Temp. **44**, 308–313 (March 2018)

SQUID magnetometers for biomagnetic measurements are equipped with superconductive gradiometers which are required to provide a high signal-to-noise ratio at low frequencies, sufficient mechanical strength and sustained performance under repeated thermal cycles, as well as a low level of intrinsic magnetic noise. This paper describes the design of a gradiometer made with a carbon-fiber reinforced composite material for magnetic cardiography measurements. The thermal coefficient of linear expansion (TCLE) of the carbon fiber composite can be precisely adjusted to match that of the superconducting detector coil wire. This is achieved thanks to the difference in the TCLE of carbon fibers in the longitudinal and transverse directions and is realized by varying the laying directions of the fiber in the composite. The data of magnetic susceptibility measurements on carbon fiber composite are reported, showing the magnetic susceptibility about six times smaller than that of graphite. The presented gradiometer design provides a high degree of balancing and is patented along side other specific techniques. *Published by AIP Publishing.*
https://doi.org/10.1063/1.5024543

Introduction

Modern SQUID magnetometers have the ultimate sensitivity to changes in magnetic flux, which is determined by the intrinsic noise of the SQUID and the signal transfer coefficient from the sample to the magnetic flux transformer and further to the interferometer. Such magnetic flux transformers, often referred to as antennas, can be made in the form of superconducting gradiometers—a serial connection of several coils made of wire (axial) or films deposited on a substrate (planar).[1] They improve the signal-to-noise ratio at the input of the magnetometer and allow to achieve a magnetic field resolution in the pT and fT range.

For measurement objects in close proximity, located at a distance R of the order of the distance between the coils (the base of the gradiometer), the attenuation of the useful signal is insignificant, while a signal from distant sources of magnetic interference is suppressed as $1/R^{(3+M)}$, where M is the gradiometer order and R is the distance to the source of interference (Fig. 1).

When performing measurements on biological objects, for instance, measuring cardiology spectra, a useful magnetic signal from the measurement objects is concentrated in the low-frequency range 0.1–100 Hz. The general noise environment in which real objects are measured is determined by the presence of industrial sources of magnetic interference (broadcasting stations, mobile communications, electrostatic discharges, as well as other sources of electromagnetic fields and waves). Their intensity is manyfold higher than the useful extremely weak magnetic signal, and their significant attenuation (1000 times and more) is achieved only with a sufficiently accurate manufacture of the gradiometer and is also determined by its design and structural materials.[2]

Design features of the gradiometer

The construction of a second-order wire gradiometer[3] is shown in Fig. 2 and includes a cylindrical body *1*, detection coil *5* and two compensation coils *2* and *4* wound on a cylindrical body with a single superconducting wire and connected by forward and backward pieces of wire *3* wound together and embedded in a vertical groove. The compensation coil *4* is a two-turn coil located in the middle of the housing; the detection coil and second compensation coil are single-turn coils located at the opposite ends of the housing.

Turns of all the coils are located in annular groves, the planes of which are instrumentally perpendicular to the axis of the gradiometer housing. The turns of the coils should be spaced at a distance not less than half their radius. In this design, this distance is $B = 60$ mm with the center-line diameter of the detection coil $D = 20$ mm. This design provides an initial unbalance of 400–800 (200–400) ppm for the vertical (horizontal) field component. The advantage of this design is a sufficient (about 20 ppm after mechanical balancing) level of attenuation of magnetic interference along the vertical component of the magnetic field, which contains a useful signal.[4]

The antenna housing also has three holes necessary for the installation of a three-axes gradiometer balancing

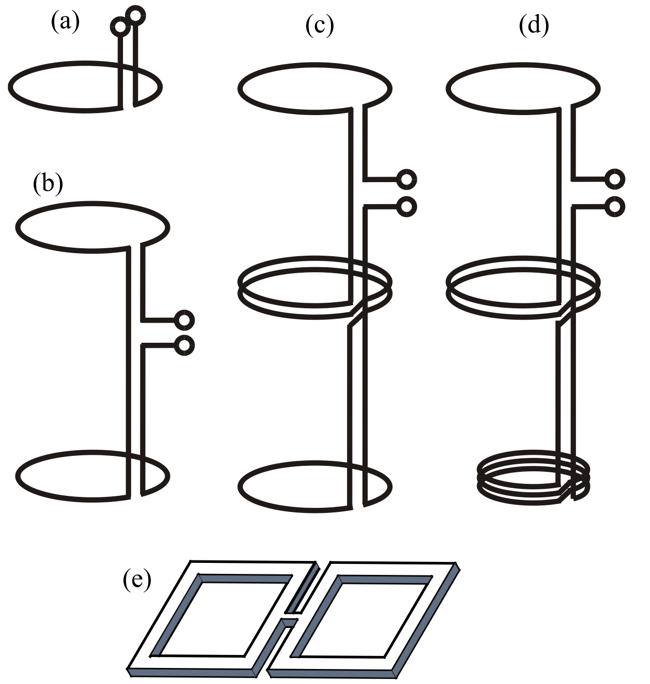

Fig. 1. Different types of gradiometric antennas: magnetometer (a); first-order gradiometer (b); symmetric second-order gradiometer (c); asymmetric second-order gradiometer (d); planar first-order gradiometer (e).

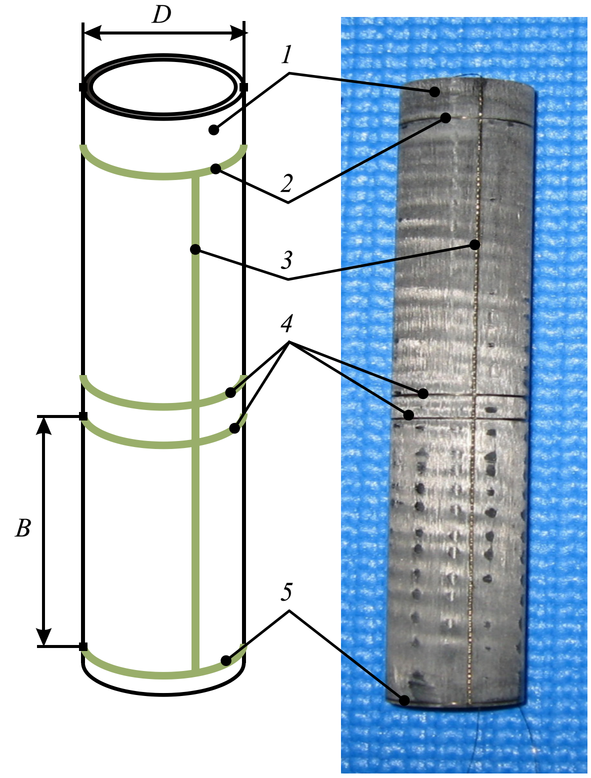

Fig. 2. Image of a second-order gradiometer with a carbon-fiber frame.

mechanism with tuning elements made of lead. The balancing procedure consists in shifting these elements relative to the antenna coils until their effective areas coincide.

This design allows not only to reduce the vertical component of magnetic noise but also the noise gradient from distant sources. This is manifested in a decrease in the cutoff frequency of the $1/f$ noise in the spectrum of the output signal of the magnetometer from 10 Hz to 0.4 Hz. Figure 3 shows the dependence of the spectral density of the ambient background radiation measured in a fiber-glass cryostat using a second-order gradientometer based on the CARDIOMOX MCG9 cardiomagnetic system. Figure 4 shows a more detailed spectrum of the background signal in the low-frequency region to illustrate the $1/f$ noise range.

In the development of antenna housings, a number of structural materials can be used, however considerable experimental experience has already been accumulated, and the requirements to the gradiometer design have been determined. Thus, the practice of using housings fabricated from various types of fabric-resin laminates, plastics, or dense graphite has revealed a number of shortcomings. These are primarily the low mechanical strength of the antenna housing and the change in antenna balancing during thermal cycling due to the different behavior of the thermal coefficient of linear expansion (TCLE) of the housing material and wire during cooling. Therefore, in this paper we propose the design of a gradiometer that simultaneously provides mechanical strength, a high degree of attenuation of magnetic interference, and stability of characteristics under repeated cooling-warming cycles during operation.

Constitutive properties of a composite

Carbon fibers are characterized by extremely high values of the elasticity modulus and strength, chemical and thermal resistance, low coefficient of linear thermal expansion, particular tribological properties, enhanced (compared to other fibers) heat and electrical conductivity, as well as a number of other important properties. The whole range of their useful characteristics is determined both by the nature of the source material and by the variety of structural features.[5] The electrical resistivity, depending on the conditions of production, can vary by nine orders of magnitude. The thermal coefficient of linear expansion can take not only positive but

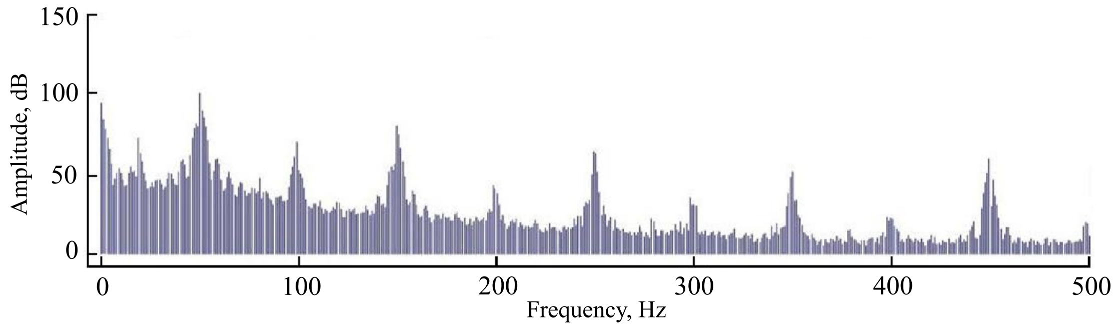

Fig. 3. Logarithmic spectrum of the flux noise density of a CARDIOMOX MCG9, 9-channel magnetic cardiology scanner (Oxford Science Park, August 16, 2017).

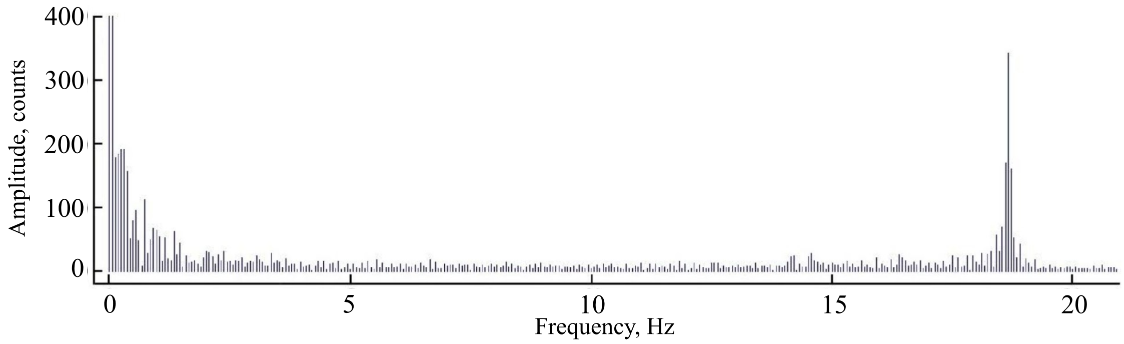

Fig. 4. Linear spectrum of the flux noise density of a CARDIOMOX MCG9, 9-channel magnetic cardiology scanner (Oxford Science Park, August 16, 2017).

also negative values. This can be explained by the fact that carbon fibers themselves have a layered structure. These layers are predominantly oriented along the fiber, i.e., in a direction perpendicular to the main crystallographic axis, similar to graphite, which results in a negative value of the TCLE along the fiber. Across a carbon fiber, as in graphite, the TCLE along the crystallographic axis is positive and greater than the absolute value of the TCLE of the fiber in the longitudinal direction.

Using the simple structure of the composite, it can be represented by repetition of two layers with different directions of reinforcing fibers (Fig. 5), and the integral TCLE is determined by the equation of strain compatibility of both layers. In this case, each layer has the properties of a unidirectional composite. With a change in the temperature of the composite material, there are stresses appearing in the layers due to the strain compatibility: compressive stresses in one layer and tensile stresses in another one. Linear deformation of the material in each layer is described by Hook's law, and the volume content of binder and fibers in each layer is provided by technological equipment and is the same over the cross section of the composite. Then a different number of fibers in the layers is achieved by different thicknesses of these layers.

For each layer of a composite with an ordered fiber direction, the expressions[6] for TLCE along $\alpha_{||}$ and across $\alpha_{\perp}$ the fiber direction:

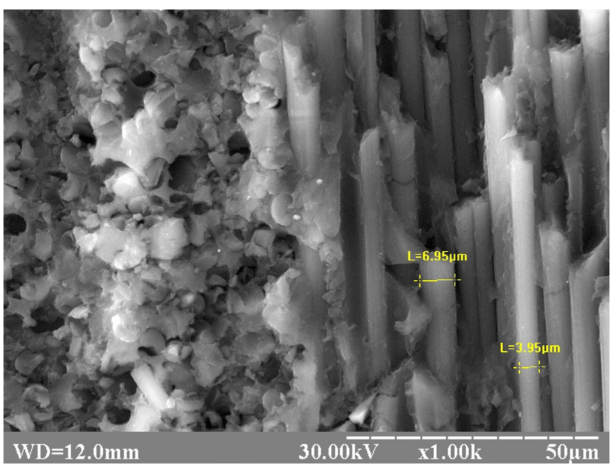

Fig. 5. Carbon fiber composite fractured at the interface of two layers with different orientation of carbon fibers. The micrograph was acquired with a REM106I scanning electron microscope.

$$\alpha_{||} = \alpha_f + (\alpha_m - \alpha_f)\Big/\left[1 + \left(\frac{\nu_f}{1-\nu_f}\right)\frac{E_f}{E_m}\right], \tag{1}$$

$$\alpha_{\perp} = \alpha_m - (\alpha_m - \alpha_f)\left\{[2(1+\mu_m)(\mu_m^2 - 1)C] \Big/ \left(\frac{1+1,1\nu_f}{1,1\nu_f - 1} - \mu_m + 2\mu_m^2 C\right) - \left(\nu_m \frac{E_f}{E_m}\right)\Big/\left(\frac{1}{C} + \frac{E_f}{E_m}\right)\right\}. \tag{2}$$

The constant C in Eq. (2) for cylindrical fibers is $C = 1.1\nu_f\,(1 - 1.1\,\nu_f)$ and α_m, α_f, E_m, E_f, ν_m, ν_f are TLCE, Young's moduli, the bulk content for the polymer matrix (index m) and fibers (index f) in the composite, respectively; μ_m is the Poisson's ratio of the polymer matrix.

From this it can be seen that the TLCE of a composite is governed both by the relative content of the binder in the material and its type and the relative amount of reinforcing fibers in the layers and their orientation. For a cylindrical antenna frame, the total TLCE of the composite material with multiple layers of unidirectional fibers is calculated. In the case of orthotropic reinforcement, when the orientation of the fibers is along the axis of the frame in one layer and transverse in another layer, the resulting $\alpha_{C\perp}$ determines the radial deformation while $\alpha_{C||}$ determines the axial and angular deformations.

Proceeding from the need to make a frame with a wall thickness not exceeding 1.0 mm, a technological process was developed using an ED-22 epoxy resin reinforced with VMN-4 high-strength carbon fibers. From the reference data on these materials,[5,7] we have for carbon fibers: $E_{||} = 240$ GPa, $\alpha_{||} = -0.9 \times 10^{-6}\ \mathrm{K}^{-1}$, $E_{\perp} = 6.7$ GPa, and $\alpha_{\perp} = 75 \times 10^{-6}\ \mathrm{K}^{-1}$. Then, based on the strain compatibility theorem, a system of linear equations for two layers with unidirectional fibers is written, and we obtain the dependence of the components of the integral thermal coefficient on the relative thicknesses of the layers, i.e., on the amount of fibers in different directions (Fig. 6).

Since the imbalance of a gradiometer occurs upon the displacement of the transverse turns of the antenna, it is therefore necessary to achieve equal thermal deformation of the housing in the angular and axial direction ($\alpha_{C||}$) and that of the wire material $\alpha_{\mathrm{Nb}} = 7.1 \times 10^{6}\ \mathrm{K}^{-1}$.[8] It can be seen that the choice of such materials provides significant technological flexibility in the selection of the amount of fibers in the matrix and their ratio in different layers of the composite

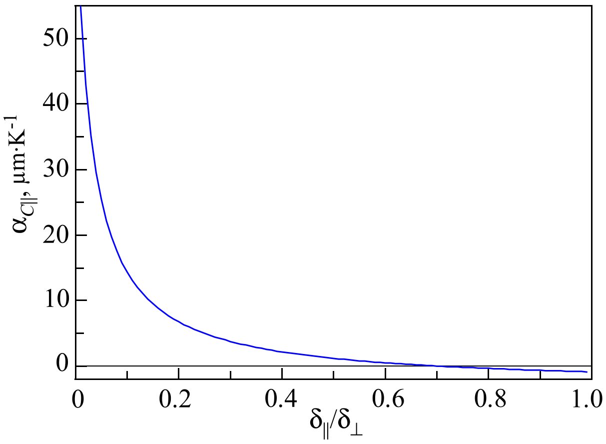

Fig. 6. Calculated dependence of the integral TCLE of the carbon fiber composite along the axis of the frame as a function of the ratio of the thicknesses of the layers with the longitudinal and transverse orientations of the carbon fibers.

material for aligning the TCLE of the composite and the wire material.

Magnetic properties of the carbon fiber composite

Experimental studies showed that the combination of these types of materials in the composite leads to a reduction in its magnetic susceptibility. Figure 7 shows the magnetic susceptibility of graphite (triangles) and carbon fiber composite (circles) in the temperature range 5–50 K. The measurements were carried out using a laboratory susceptometer with a sensitivity to the magnetic moment no worse than 4×10^{-10} A m^2, which allowed to conduct precise measurements using an SGM-5 SQUID magnetometer.[9]

The measurements on the carbon fiber composite were carried out using the magnetic susceptibility data for a graphite frame taken from a previously used gradiometer as a reference.

Figure 7 shows that with lowering temperature, the magnetic susceptibility of both materials increases and at $T = 5$ K becomes equal to -2.27×10^{-5} (SI units) for graphite and $+3.89 \times 10^{-6}$ (SI units) for carbon fiber composite. Thus, the experimental data indicate that graphite is a diamagnetic material and the carbon fiber composite is a paramagnetic material, but the susceptibility of the composite material is about 5.8 fold lower in absolute value. According to the authors, this is explained by mutual compensation of the

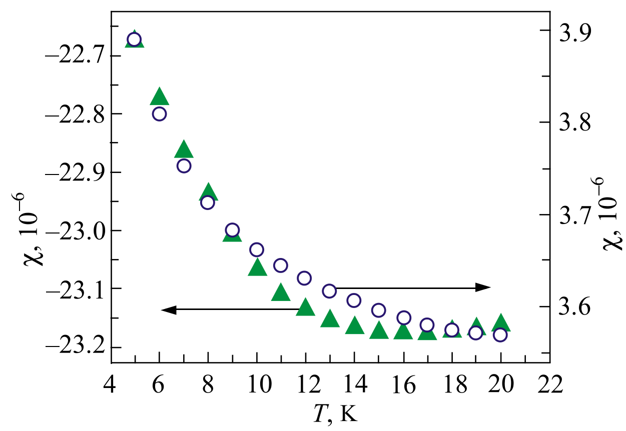

Fig. 7. Temperature dependence of the magnetic susceptibility in a constant magnetic field $B = 20$ mT for graphite (▲) and carbon fiber composite (○) measured in units SI.

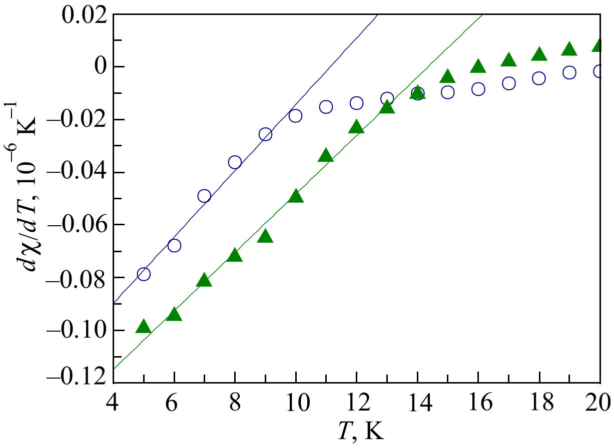

Fig. 8. Temperature dependence of the derivative of magnetic susceptibility for graphite (▲) and carbon fiber composite (○) in a constant magnetic field of 20 mT.

paramagnetism of epoxy resin and the diamagnetism of carbon fibers.

Thus, use of the composite material for the gradiometer frame reduces the magnetic distortions of the useful signal several-fold. In addition, the internal magnetic noises of the frame arising due to temperature fluctuations during boiling of liquid helium is also decreased, as can be seen in Fig. 8, which shows the temperature dependence of the temperature derivative of magnetic susceptibility for both materials.

Let us quantify the magnetic interference generated by the antenna frame by finding the magnetic moment fluctuations dM produced by a material of volume V in a magnetic field H upon temperature variations dT

$$dM = \frac{d\chi}{dT} VHdT. \tag{3}$$

For a material with a volume of 1 cm^3 at a temperature $T = 4.2$ K and temperature fluctuations due to the boiling of helium $dT = 10^{-4}$ K in the Earth's magnetic field $H = 50$ mT, we obtain from the experimental data shown in Fig. 8, $d\chi/dT = -1.13 \times 10^{-5}$ K^{-1} for graphite and $d\chi/dT = -0.9 \times 10^{-5}$ K^{-1} for carbon fiber composite. Thus, according to Eq. (3), the magnetic moment fluctuations are $dM \approx 5.65 \times 10^{-20}$ Wb·m for graphite and $dM \approx -4.5 \times 10^{-20}$ Wb·m for carbon fiber composite, i.e., the magnetic interference from carbon fiber composite is 1.3 times lower than that of graphite.

Specific implementation

The technology of manufacturing the carbon-fiber frame for a gradiometer was developed for the application in four 9-channel cardiomagnetic scanners CARDIOMOX MCG9, produced during 2015–2017 in Glushkov Institute of Cybernetics NASU (Kiev) within the project R624 of Science and Technology Center in Ukraine. The device employs a number of unique inventions protected by international and national patents.[10–16]

Conclusions

The main advantage of this design is the practical absence of mechanical deformations and shifts of the detection coils caused by thermal expansion of materials. This ensures that the position and area of the gradiometer coils remain unchanged, which in turn ensures the stability of the antenna unbalance under repeated thermal cycles between liquid helium and room temperatures.

This makes it possible to achieve an initial unbalance of 800 ppm in the axial component of the field and 400 ppm in the transverse direction, which is sufficient for ultra-sensitive measurements under unshielded conditions without the use of additional interference suppression (adaptive interference compensation, magnetically shielded room or enclosure). An additional advantage of the composite is its better magnetic properties (six times lower magnetic susceptibility), which provides less distortion of the useful signal.

The value of the specific bulk electrical resistance of carbon fiber composite measured by the four-probe method was $3.5 \times 10^{-4}\ \Omega$ m. This is approximately 20 times higher than that of the graphite used earlier, which ensures a significant absorption of high-frequency electromagnetic interference.

[a]Email: budnyk@meta.ua

[1]S. D'Angelo, I. Modena, and G. L. Romani, U.S. patent US4523147A (1985).
[2]A. Bakharev, International patent application WO2002027332 (2002).
[3]Yu. D. Minov, M. M. Budnyk, and Kiev Medical Group Ltd., Ukrainian patent for invention UA16882 (2006).
[4]Yu. D. Minov and M. M. Budnyk, International patent application WO2012173584 (2012).
[5]A. I. Meleshko and S. P. Polovin, *Carbon, Carbon Fibers and Carbon Composites* (Science Press, Moscow, 2007) [in Russian].
[6]A. B. Kruglov, "Thermophysical properties of glass epoxides and epoxy resins at cryogenic temperatures," PhD thesis, Moscow (2007) [in Russian].
[7]S. Simamura, A. Sindo, K. Kotsuka, N. Tsutiyama, T. Sato, Y. Ito, K. Ikegami, K. Yamada, A. Sakamoto, Y. Vatanabe, H. Takeda, T. Isikawa, V. Sasaki, and Y. Abe, *Carbon Fibres* (Omsya, Tokyo, 1984) (in Japanese); [Russian translation: (Mir, Moscow, 1987)].
[8]M. P. Malkov, I. B. Danilov, A. G. Zeldovich, and A. B. Fradkov, *Handbook of Physical and Engineering Fundamentals of Cryogenics* (Energoatomizdat, Moscow, 1985) [in Russian].
[9]A. V. Fedorchenko, V. Yu. Lyakhno, and V. I. Shnyrkov, Vopr. At. Nauki Tekh., Ser. Fiz. Radiats. Povredhdenii Radiats. Materialoved. **1**(65), 150 (2010) [in Russian].
[10]V. M. Sosnytskyy, Yu. D. Minov, and M. M. Budnyk, International patent application, WO2013115749 (2013).
[11]V. M. Sosnitskii, Yu. D. Minov, and M. M. Budnik, Ukrainian patent for invention, UA102163 (2013).
[12]Yu. D. Minov, M. M. Budnyk, V. Yu. Lyakhno, O. B. Shopen, and O. B. Kivirenko, International patent application, WO2016114742 (2016).
[13]Yu. D. Minov, M. M. Budnyk, V. Yu. Lyakhno, O. B. Shopen, and O. B. Kivirenko, Ukrainian patent for invention, UA112235 (2016).
[14]M. Budnyk, N. Dudchenko, O. Stavynska, Yu. Alekseytsev, O. Dudchenko, I. Chaikovsky, Yu. Minov, P. Sutkovyi, P. Shpylyovy, and T. Ryzhenko, Materialwiss. Werkstofftech. **40**, 302 (2009).
[15]M. Budnyk, O. Zakorcheny, V. Budnyk, V. Koshelnyk, V. Lukashyk, Yu. Minov, P. Sutkovyi, and T. Ryzhenko, in *IFMBE 28 Proceedings Series* (Springer Verlag, Berlin, 2010).
[16]M. Budnyk, V. Sosnytskyi, I. Voitovych, V. Maiko, Yu. Minov, P. Sutkovyi, O. Zakorchenyi, T. Ryzhenko, and V. Budnyk, in Proceedings of the IEEE 6th Workshop "Intelligent Data Acquisition & Advanced Computing Systems IDAACS" 2011, Prague (2011).

Translated by L. Gardt